

See discussions, stats, and author profiles for this publication at: <https://www.researchgate.net/publication/263947291>

# Recycling Agricultural Waste from Palm Shells during Electric Arc Furnace Steelmaking

ARTICLE *in* ENERGY & FUELS · OCTOBER 2011

Impact Factor: 2.79 · DOI: 10.1021/ef201184h

---

CITATIONS

13

READS

100

## 6 AUTHORS, INCLUDING:



Nur Farhana Diyana Mohd Yunos

Universiti Malaysia Perlis

14 PUBLICATIONS 21 CITATIONS

[SEE PROFILE](#)



Asri Idris

Universiti Malaysia Perlis

9 PUBLICATIONS 25 CITATIONS

[SEE PROFILE](#)



Rita Khanna

University of New South Wales

106 PUBLICATIONS 442 CITATIONS

[SEE PROFILE](#)



Veena Sahajwalla

University of New South Wales

148 PUBLICATIONS 772 CITATIONS

[SEE PROFILE](#)

# 1 Recycling Agricultural Waste from Palm Shells during Electric 2 Arc Furnace Steelmaking

3 Nur Farhana M. Yunos,<sup>\*,†,‡</sup> Magdalena Zaharia,<sup>†</sup> M. Asri Idris,<sup>‡</sup> Dilip Nath,<sup>†</sup> Rita Khanna,<sup>†</sup> and  
4 Veena Sahajwalla<sup>†</sup>

5 <sup>†</sup>Centre for Sustainable Materials Research and Technology (SMaRT@UNSW), School of Materials Science and Engineering,  
6 The University of New South Wales, Sydney, New South Wales 2052 Australia

7 <sup>‡</sup>School of Materials Engineering, The University of Malaysia Perlis, Kubang Gajah 02600, Perlis, Malaysia

**ABSTRACT:** The present study is focused on developing novel recycling of palm shell wastes as a carbon resource in electric arc furnace (EAF) steelmaking. Metallurgical coke was replaced by palm shells, and interactions with EAF slag were investigated at 1550 °C in a laboratory-scale reactor using the sessile-drop approach in an argon atmosphere (1 L/min). The palm shells were devolatilized in a nitrogen atmosphere at 450 °C, while coke was used without initial processing. The quantitative estimation of the slag droplet volume was performed using the  $V_t/V_0$  ratio as a measure of slag foaming. For coke, the volume ratio decreased from 1.0 to 0.8 in the first 10 min with no considerable fluctuations. However, palm shell char showed considerably different trends with continuous fluctuations, reaching a maximum value of  $V_t/V_0 = 1.3$ , indicating a higher extent of gas entrapped into the slag matrix compared to coke. Off-gas emissions were monitored and correlated with dynamic changes in volume as a result of iron-oxide-rich EAF slag and carbon. The rates of total gas generation ( $\text{CO} + \text{CO}_2$ ) from palm shell char were comparable to those seen in coke; however, the gases released from palm shell were an extent over a longer period of time, which allowed for their entrapment in the slag matrix, enhancing the volume of the slag. A thermogravimetric analyzer coupled with a mass spectrometer (TGA–MS) was used to study the behavior of coke and palm shells at high temperatures, with a focus on gas formation. The weight loss profiles, gas formation, and product distribution were significantly different between the two carbonaceous samples. It was found that more gases were released from palm shells than from the raw coke. Palm shells showed significant weight loss in the first 500 °C; however, a considerable amount of gases was evolved at temperatures higher than 1000 °C that might participate in the subsequent carbon/slag reactions. Optical microscopy images of the cross-section of the slag/palm shell sample showed trapped gas bubbles and reduced iron dispersed throughout the slag matrix. These results indicate that partial replacement of coke with palm shells is not only viable but efficient, leading to improved/sustained interactions with EAF slag.

## 1. INTRODUCTION

Agricultural waste materials derived from palm shells are among the main renewable waste source in Malaysia. Approximately 2.01 million tons of palm shells were generated in 2010 alone, and a steady 5% increase has been seen in the past few years.<sup>1,2</sup> Because of global environmental concerns over excessive fossil fuel usage (coal) in the iron and steel industry, sustainable biomass resources have grown in importance as partial alternatives to fossil resources. It is reported that approximately 2 tons of  $\text{CO}_2$  emissions are generated per ton of steel by the iron and steel industry.<sup>3,4</sup> These emissions can be reduced by substituting renewable carbon materials derived from agricultural waste materials, because the cellular carbon in these wastes is derived from the usage of carbon dioxide in the atmosphere in the photosynthesis process.<sup>5</sup>

In the ironmaking and steelmaking industries, the use of biomass/agricultural waste as a supplementary source alongside coal has attracted interest. The use of wood char in ironmaking has been extensively reviewed by Gupta,<sup>6</sup> Burgess,<sup>7</sup> and Dell'Amico et al.<sup>8</sup> Charcoal has been used as a reducing agent in blast furnaces for a number of years.<sup>9,10</sup> Babich et al.<sup>11</sup> found that the combustion efficiency of all of the tested charcoals is better or comparable to conventional coals. The use of palm shell charcoal for the production of good quality steel was considered by

Emmerich et al.<sup>12</sup> because of the low amounts of sulfur and phosphorus present in this agricultural waste. Furthermore, the palm shell waste is a renewable material, which does not contribute to the increase in the global  $\text{CO}_2$  concentration.<sup>13</sup> Recently, a carbon–iron ore composite consisting of biomass char coated with sub-micrometer iron oxide powder and iron ore fines was proposed to improve the reduction rate in the blast furnace.<sup>14</sup> Most of the previous studies have been carried out using biomass as a reduction agent in a blast furnace, while less investigation was considered for applications in electric arc furnace (EAF) steelmaking. The present study is focused on carbon/slag interactions between an EAF slag and palm shell as carbon material.

One of the important carbon/slag interactions in EAF steelmaking is slag foaming that involves the entrapment of gas bubbles in the slag layer when carbon-based materials interact with iron oxide in the slag. This gas foams the slag, creating more volume depending upon parameters, such as slag characteristics,

**Special Issue:** 2011 Sino-Australian Symposium on Advanced Coal and Biomass Utilisation Technologies

**Received:** August 2, 2011

**Revised:** October 5, 2011

**Table 1.** Proximate and Ultimate Analyses of MC and Palm Shell Char Samples

|                 | proximate analysis (% db) |              |      |          | ultimate analysis (% db) |      |      |      |      |
|-----------------|---------------------------|--------------|------|----------|--------------------------|------|------|------|------|
|                 | volatile matter           | fixed carbon | ash  | moisture | N                        | C    | H    | O    | S    |
| MC              | 6.1                       | 73.2         | 17.2 | 3.5      | 2.41                     | 80.4 | 1.13 | 15.7 | 0.36 |
| palm shell char | 33.6                      | 56.6         | 5.6  | 4.2      | 0.58                     | 76.5 | 5.73 | 17.5 | 0.05 |

**Table 2.** Ash Analysis of the Carbonaceous Materials Used in This Study (wt %)

| compound                       | MC (%) | palm shell char (%) |
|--------------------------------|--------|---------------------|
| SiO <sub>2</sub>               | 57.4   | 51.6                |
| Fe <sub>2</sub> O <sub>3</sub> | 5.9    | 21.7                |
| Al <sub>2</sub> O <sub>3</sub> | 26.5   | 6.8                 |
| TiO <sub>2</sub>               | 1.2    | 0.27                |
| P <sub>2</sub> O <sub>5</sub>  | 0.6    | 1.88                |
| Mn <sub>3</sub> O <sub>4</sub> | 0.3    | 0.38                |
| CaO                            | 4.1    | 2.41                |
| MgO                            | 0.6    | 2.18                |
| Na <sub>2</sub> O              | 0.2    | 5.6                 |
| K <sub>2</sub> O               | 0.7    | 5.6                 |
| SO <sub>3</sub>                | 2.5    | 1.68                |

carbon material employed, amount of oxygen injected, FeO content in the slag, temperature, etc. The slag foam develops around the electrodes and submerges the arc, thus protecting the refractory walls from arc radiation and reducing the heat losses from the bath. The noise level, fume emission, and baghouse load are reduced as both the bath and the arc are submerged in foaming slag.<sup>15</sup> Benefits because of the slag-foaming practice have been widely reported in the literature.<sup>16</sup> The main criteria for slag foaming is to contain gas bubbles in the slag layer for a specific period of time.<sup>17,18</sup> Previous studies reported in the literature were mostly concerned with the foaming behavior of slag in a steady state, where foam was generated by bubbling gas through a nozzle.<sup>19</sup> Research from our group has shown that waste plastics and rubbers can be used as a source of carbon for slag foaming in EAF steelmaking.<sup>20–23</sup>

Although a number of studies on carbon/slag interactions have been carried out, the current understanding of the characterization behavior of material used for slag foaming and the time-dependent growth of reaction products are limited. This study will focus on the characterization of the carbonaceous materials, i.e., coke and palm shell char, using thermogravimetric analysis combined with mass spectroscopy (TGA–MS) to determine the thermal degradation of the material as well as gas formation at high temperatures. This research is important to understand the subsequent carbon/slag reactions. The sessile-drop method was used to study the *in situ* reactions taking place at steelmaking temperatures  $T = 1550\text{ }^{\circ}\text{C}$ . The present study involves a quantitative estimation of the changes occurring in the slag volume as a function of time: measurements of gas generation (CO and CO<sub>2</sub>) as a result of high-temperature carbon/slag reactions and determination of the entrapped gases and reduced metal by means of optical microscopy.

## 2. EXPERIMENTAL SECTION

### 2.1. Material Characteristics.

Two carbonaceous materials, metallurgical coke (MC) and palm shell char, were used in this study.

**Table 3.** Chemical Composition of the EAF Slag (wt %)

| EAF slag composition           | wt % |
|--------------------------------|------|
| Fe <sub>2</sub> O <sub>3</sub> | 34.9 |
| CaO                            | 30.4 |
| Al <sub>2</sub> O <sub>3</sub> | 6.9  |
| MgO                            | 10.9 |
| SiO <sub>2</sub>               | 11.6 |
| MnO                            | 5.0  |

Proximate/ultimate and ash analyses of these materials are presented in Tables 1–3. Palm shell char was prepared by devolatilization at 450 °C of the palm shell waste in a N<sub>2</sub> atmosphere to remove its volatile matter.<sup>24</sup> The carbonaceous substrates were prepared by grinding and sieving the carbon-based materials to particle sizes <60 μm and further compacting them at ~4.0 MPa in a steel die using a hydraulic press. The substrate had a diameter of 20 mm and a thickness of 3–4 mm. The substrate was placed on an alumina holder of the sessile-drop experimental assembly, and the carbon/slag reactions were recorded by a charge-coupled device (CCD) equipped with a video camera.<sup>25</sup>

**2.2. Thermogravimetric Analysis (TGA).** The powdered samples of the individual palm shell waste and coke were subjected to TGA under non-isothermal conditions to continuously monitor the evolution of gases released over a wide range of temperatures (0–1450 °C). The TGA experiments were performed simultaneously using a thermogravimeter (STA 449 F1 Jupiter, Netzsch Instruments, Inc.) and a quadrupole mass spectrometer (MS; QMS 403 Aélos) connected to a thermobalance, where three coaxial tubes were used for the connection of the two instruments. The inner tube is a capillary transfer line connected to the MS detector ion source. The outer tube is connected to a vacuum source to produce stable laminar flow conditions. The sampling period and duration are adjusted by an electronically controlled solenoid valve. The inert gas used was helium with a flow rate of 0.1 L/min in the thermobalance. The samples, approximately 6 mg, were heated in the thermobalance from 0 to 1450 °C with a rate of 10 °C min<sup>-1</sup>. The intensity of the following selected ions at  $m/z$  2 (H<sub>2</sub><sup>+</sup>),  $m/z$  15 (CH<sub>3</sub><sup>+</sup>),  $m/z$  16 (CH<sub>4</sub><sup>+</sup>),  $m/z$  18 (H<sub>2</sub>O),  $m/z$  27 (HCN),  $m/z$  28 (CO),  $m/z$  28 (N<sub>2</sub><sup>+</sup>),  $m/z$  30 (C<sub>2</sub>H<sub>6</sub><sup>+</sup>),  $m/z$  40 (C<sub>3</sub>H<sub>4</sub><sup>+</sup>),  $m/z$  40 (NO), and  $m/z$  44 (CO<sub>2</sub>) was continuously detected with thermogravimetric parameters (temperature, time, and mass).

**2.3. Carbon/Slag Interactions.** Sessile-drop investigations on the carbon/slag reactions were carried out at 1550 °C in a laboratory-scale, horizontal tube furnace.<sup>26</sup> This technique was shown that it can be used to continuously monitor the changes in droplet volume (a measure of gas entrapment and, therefore, slag foaming) as a function of time.<sup>27</sup> A schematic diagram of the experimental setup is shown in Figure 1.

The sample assembly consisting of an alumina specimen holder was kept in the cold zone of the furnace until the desired temperature (1550 °C) was attained. Further, it was inserted into the hot zone of the furnace. This eliminated any reaction that could occur at lower temperatures that would influence the phenomena to be studied at the temperature of interest. The weight of the slag was established to be ~0.065 g. Off-gases evolved at the reaction temperature (CO and CO<sub>2</sub>)

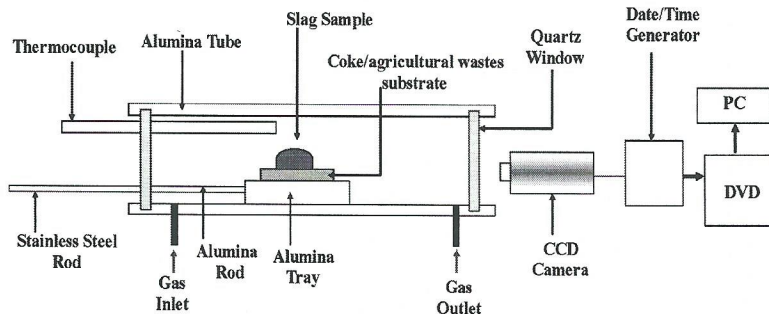


**Figure 1.** Schematic diagram of the sessile-drop apparatus.

were monitored using an infrared (IR) analyzer. A time delay of about 60 s was required as the time needed for the gas to travel from the hot furnace to the gas analyzer, as well as the time needed for the substrate and slag to reach the reaction temperature.<sup>21</sup> The gas data were used to determine the total amount of gases (moles), which evolved from the reacting samples as a function of time. Argon gas (99.99% purity, 2 ppm oxygen) was used in the experiment at a flow of 1 L/min.

The melting of slag marked the beginning of the reactions. A CCD camera fitted with an IRIS lens was used to capture the live *in situ* phenomena in the furnace, and a digital video disk (DVD) recorder connected to the television allowed for the recording of the entire experiment as a function of time. Dynamic changes in volume were determined from the captured images with the help of computerized data-processing software. As an approximation, the slag droplet on the substrate was assumed to have a truncated spherical shape. Minor deviations from a spherical shape caused by continuous or sudden evolution of gases were neglected (estimated error of  $\sim 5$  vol %).<sup>27</sup> The sessile-drop slag-foaming software<sup>27</sup> generates the volume ratio " $V_t/V_0$ " as a function of time, where  $V_t$  and  $V_0$  represent the volume at time  $t$  and the volume of the slag at the initial stage, respectively.

**2.4. Microscopic Investigations.** Optical microscopic observations were carried out on the interfacial region of the reacted carbon/slag assemblies. Once the sample was pushed in the hot zone and the counter was started, the slag droplet started to melt and the reaction time was closely monitored. The tray containing the slag droplet and the carbon substrate were withdrawn into the cold zone of the furnace at regular time intervals. Samples were collected for the following times: 1, 2, 10, and 20 min. For microscopic investigations, the quenched carbon/slag assembly was set in an epoxy resin mold; the set assembly was then sectioned carefully, exposing the vertical cross-section of the carbon substrate/slag assembly, and was reset in the mold. After final polishing, the samples were dried at 60 °C for 12 h to remove the moisture. These samples were used to investigate the formation of reduced metal as a result of an iron oxide reduction and the distribution of gas bubbles trapped within the slag droplet.

### 3. RESULTS AND DISCUSSION

**3.1. Effect of the High Temperature on the Behavior of the Carbonaceous Substrate.** Carbon is continuously injected into the slag bath of the EAF, where the temperature exceeds 1500 °C. In these conditions, the initial gas-phase reactions occur very fast and the gases evolved at these high temperatures are expected to participate in the subsequent slag reactions.<sup>28</sup> The gas products evolved at high temperature were investigated using a mass spectrometer coupled to a thermogravimetric analyzer starting at room temperature and reaching up to 1450 °C.

Observed thermal behavior and gas evolution of coke during pyrolysis is shown in panels a–f of Figure 2. It was seen that coke

showing a very limited weight loss, which starts around 120 °C, was attributed to moisture release and then slowly decreases (Figure 2a). Such a behavior was expected on the basis of its composition, i.e., low volatile matter because of prior history of heat treatment. The various gaseous species detected were CO, CO<sub>2</sub>, CH<sub>3</sub><sup>+</sup>, CH<sub>4</sub><sup>+</sup>, H<sub>2</sub><sup>+</sup>, HCN, and N<sub>2</sub>. The CO peaks were observed at temperatures between 450 and 900 °C, while CO<sub>2</sub> started to evolve around 600 °C (Figure 2b). Light gases, such as CH<sub>3</sub><sup>+</sup> and CH<sub>4</sub><sup>+</sup>, were released in the temperature range of 400–650 °C (Figure 2c). HCN evolved around 350–550 °C (Figure 2f), while N<sub>2</sub><sup>+</sup> was seen in the temperature range of 400–650 °C. It is well-known that HCN is one of the main NO precursors.<sup>29</sup> These results show that MC produced higher NO emissions during pyrolysis compared to palm shells, where TGA–MS did not detect nitrogen gas released from palm shells.

Panels a–f of Figure 3 show the changes in weight loss during pyrolysis of palm shells along with the gas products (i.e., CO, CO<sub>2</sub>, CH<sub>4</sub><sup>+</sup>, CH<sub>3</sub><sup>+</sup>, C<sub>2</sub>H<sub>6</sub><sup>+</sup>, C<sub>3</sub>H<sub>4</sub><sup>+</sup>, H<sub>2</sub><sup>+</sup>, and H<sub>2</sub>O). In the experimental temperature range, the TGA curve of palm shells showed two degradation steps (Figure 3a). The first weight loss was attributed to moisture release, taking place at around 110 °C. The light gas products from the palm sample, including H<sub>2</sub><sup>+</sup>, CH<sub>4</sub><sup>+</sup>, C<sub>2</sub>H<sub>6</sub><sup>+</sup>, C<sub>3</sub>H<sub>4</sub><sup>+</sup>, CO, CO<sub>2</sub>, and H<sub>2</sub>O, were produced in the temperature range of 200–400 °C, resulting in a significant weight loss (panels a–f of Figure 3). These results are in good agreement with the previous literature that reported palm shell devolatilization occurring up to a maximum of 600 °C.<sup>30</sup> However, the present study goes beyond that, and after 950 °C, it is seen that the palm shell continues to lose weight, indicating that the gases are still being released. The proportion of H<sub>2</sub>O, CH<sub>4</sub><sup>+</sup>, and higher hydrocarbons decreased considerably, whereas the amounts of CO and CO<sub>2</sub> increased to a high extent. Hydrogen also showed an increase, however, to a lower extent. According to Yang et al.,<sup>31,32</sup> CO and CO<sub>2</sub> evolution at low temperatures are mainly caused by degradation of C=O bonds present in biomass (300–400 °C). The cracking and reforming of aromatic rings gives rise to H<sub>2</sub> that was seen at higher temperatures (>400 °C). After 950 °C, methane is expected to form CO and H<sub>2</sub>, and this might be one of the reasons behind the increase seen in CO gas (Figure 3b). Further, the reaction of water vapor with C produced from hydrocarbons cracking<sup>33–36</sup> present in palm shell releases CO and H<sub>2</sub> (panels b and d of Figure 3). The interaction of cellulose and lignin during pyrolysis was found to release H<sub>2</sub> and other hydrocarbons at 900 °C.<sup>31,37,38</sup> Palm shell contains high lignin (53.4%) and cellulose (29.7%),<sup>39</sup> and their interaction at high temperature is known to release a considerable amount of

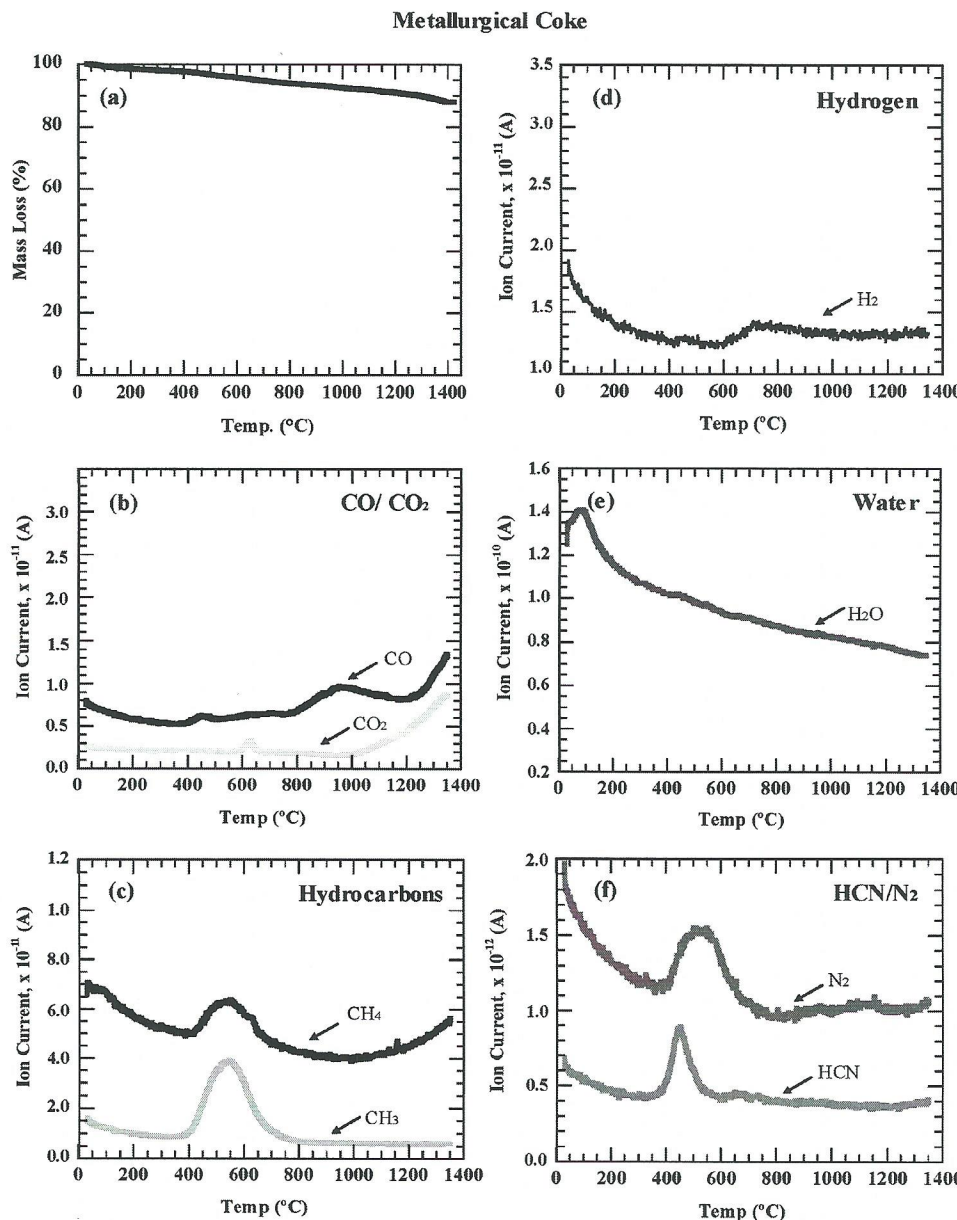
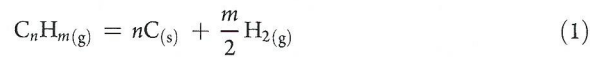


Figure 2. (a–f) Mass loss of MC with online MS analysis of the gas products during pyrolysis.

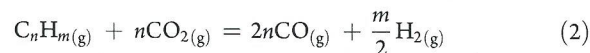
gases. Moreover, the inorganic matter could also influence the formation of gas at the temperature of 800 °C.<sup>40</sup> The palm shells are expected to improve the carbon/slag reactions because of the availability of gases, such as  $\text{CH}_4^+$ ,  $\text{H}_2^+$ , CO, and  $\text{CO}_2$ , and other hydrocarbons beyond 450 °C.

**3.2. Carbon/Slag Interactions.** 3.2.1. Off-gas (CO and  $\text{CO}_2$ ) Generation. At steelmaking temperatures (1500–1600 °C), a set of reactions (FeO reduction) are expected to occur and these have been reviewed in detail by Dankwah et al.<sup>41</sup> As the current study introduces a more complex material, palm shell char, with a different structure from that found in the conventional materials, the reactions occurring at the slag carbon interface are expected to be affected by the presence of an increased level of hydrocarbons. These hydrocarbons could further decompose into

carbon and hydrogen.<sup>41</sup>



The hydrocarbon could also act as a sink for  $\text{CO}_2$  gas to produce CO and  $\text{H}_2$ .



In the reduction of iron oxide with carbon, it is assumed<sup>42</sup> that all  $\text{Fe}_2\text{O}_3$  is first converted to FeO, followed by further reduction of FeO to Fe. The reduction of FeO to Fe takes place at a slower rate. Because the reduction of  $\text{Fe}_2\text{O}_3$  to FeO is assumed to occur quite rapidly, it has not been considered in our calculations.

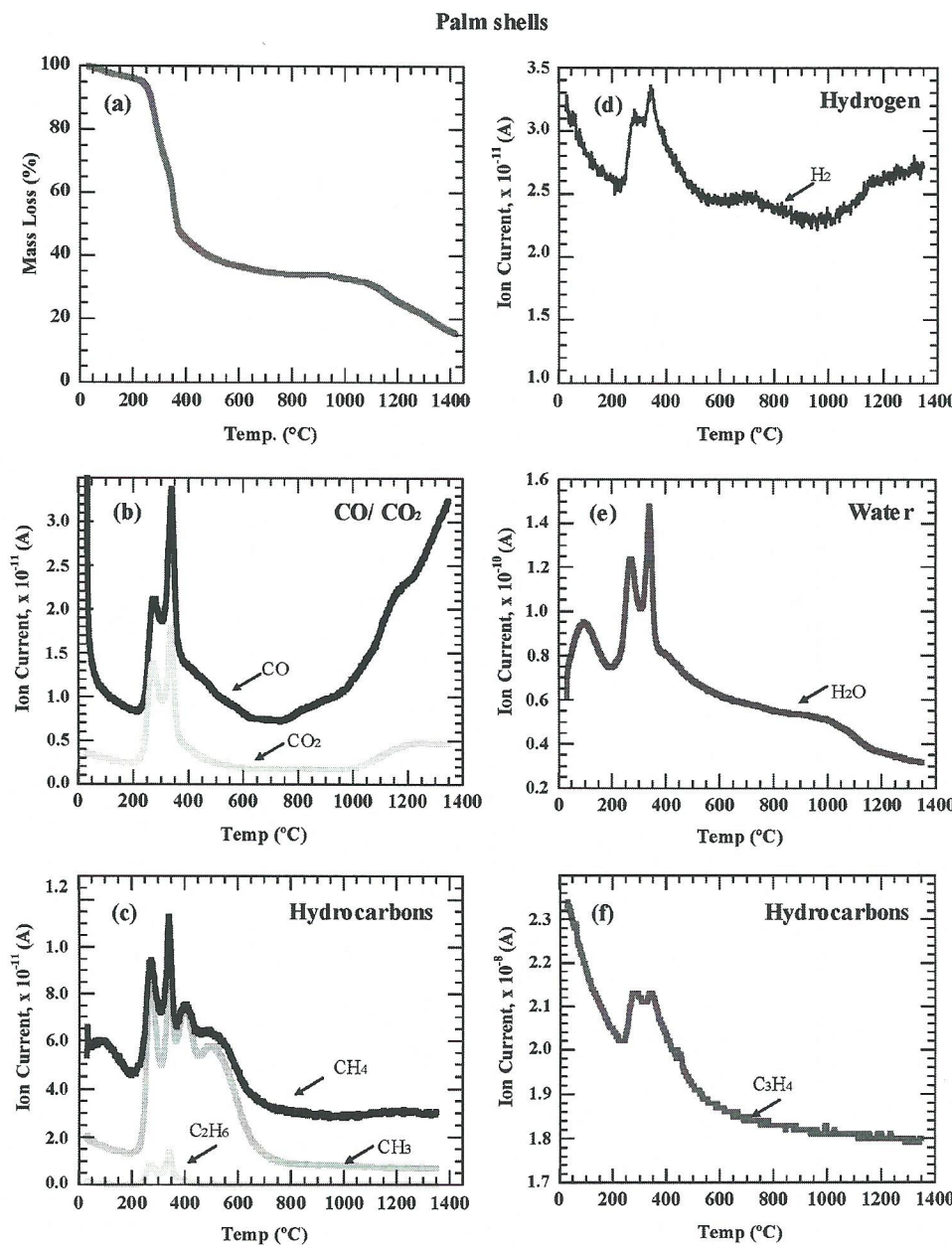
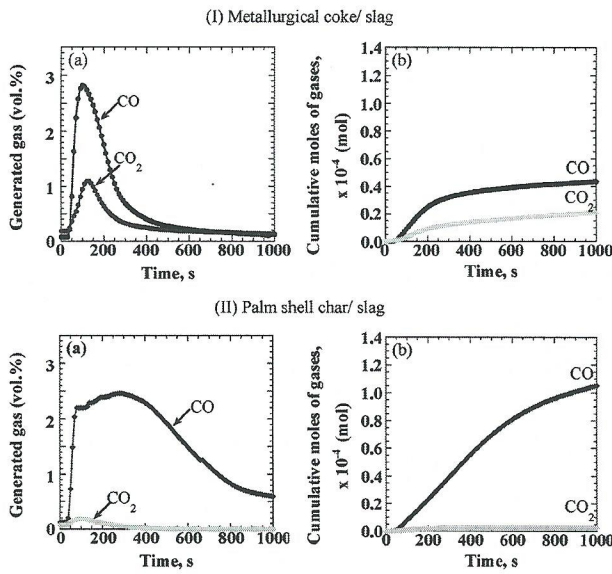


Figure 3. (a–f) Mass loss of palm shells with online MS analysis of the gas products during pyrolysis.

When put in contact with an iron-oxide-rich EAF slag, the presence of iron oxide leads to a reduction reaction depending upon the reducing agents, including C, CO, and H<sub>2</sub>, released at high temperatures. The reduction of FeO by hydrogen leads to the formation of CO, CO<sub>2</sub>, and H<sub>2</sub>O. These gases can later be found at the slag/metal interface, allowing the entire bath to become foamy. A fluctuation in volume is dependent upon the rate of gas evolution, the size of gas bubble, and the physical and chemical properties of the slag. Moreover, CO<sub>2</sub> can be produced from the reaction with H<sub>2</sub>O based on the auxiliary reaction of H<sub>2</sub>O with C to produce CO from cracking the hydrocarbon.<sup>41</sup>

Off-gas generation (CO and CO<sub>2</sub>) during the high-temperature reactions at 1550 °C between the carbonaceous substrate

and the slag (predominantly reduction of iron oxide by carbon) was determined by using IR analyzer results, as shown in Figure 4. Both panels a of I and II of Figure 4 provide volume concentrations (vol %) in terms of CO and CO<sub>2</sub> gases resulting from the interactions of the EAF slag with coke and palm shell char samples, respectively. MC showed a significant level of the carbon/slag interaction with the CO gas concentration reaching 2.8 vol % after 100 s of contact (panel a of I of Figure 4). The CO gas concentration from palm shell char/slag showed a sharp rise, attaining a value of 2.3 vol % in less than 100 s, and increased slowly thereafter, slowing after 300 s (panel a of II of Figure 4). The gradual decrease in the CO concentration is attributed to the complex structure found in palm shells breaking down at a slower



**Figure 4.** (I) MC/slag: (a) generated gas concentrations (vol %) in terms of CO and CO<sub>2</sub> gases and (b) cumulative moles of gases (mol) of CO and CO<sub>2</sub>. (II) Palm shell char/slag: (a) Generated gas concentrations (vol %) in terms of CO and CO<sub>2</sub> gases and (b) cumulative moles of gases (mol) of CO and CO<sub>2</sub>.

and steady pace. The CO<sub>2</sub> volume was seen to be significantly lower ( $\sim 0.2$  vol %) compared to than for coke (1.3 vol %) (both panels a of I and II of Figure 4). This could possibly be due to the hydrogen content present in the palm shell char ( $\sim 6\%$ ), which acts as a CO<sub>2</sub> sink.<sup>41</sup>

Both panels b of I and II of Figure 4 show the cumulative moles of gases emitted (CO and CO<sub>2</sub>) from the interaction of MC/EAF slag and palm shell char/EAF slag, respectively. The off-gases seen in MC was significantly different from the gases evolved from palm shell char. After 100 s of reaction at 1550 °C, the cumulative moles of CO gas emitted from coke was seen to increase up to  $0.5 \times 10^{-4}$  mol and, with the CO<sub>2</sub> levels, to increase up to  $0.25 \times 10^{-4}$  mol. On the other hand, CO gas emitted from palm shell char was nearly 3 times higher ( $1.15 \times 10^{-4}$  mol) than the corresponding result from coke. The total amount of CO<sub>2</sub> evolved from palm shell char was lower than the total amount of CO<sub>2</sub> gases released by coke, indicating that palm shells have a potential to reduce CO<sub>2</sub> emissions.

A higher content of oxygen present in the palm shells is an important factor in the high-temperature reactions of palm shell char with EAF steelmaking slags. The presence of oxygen in palm shells may influence CO formation at high temperatures (Figure 3b and II of Figure 4). According to some researchers,<sup>30,31</sup> the source of CO is aryl ether linkages (R—O—R) from cellulose and hemicellulose. H<sub>2</sub> peaks were also detected in the last stages of thermal decomposition (Figure 3d). H<sub>2</sub> comes from the condensation of aromatic structures (lignin) or the decomposition of heterocyclic compounds (cellulose/hemicellulose), processes that are known to occur at high temperatures.<sup>31,37,43</sup>

CO<sub>2</sub> from the coke sample (Figure 2b) is formed from aliphatic and aromatic carboxyl and carboxylate groups at low temperatures (625 °C). However, at high temperatures, CO<sub>2</sub> is derived from more thermally stable ether structures (aromatic).<sup>44,45</sup> Moreover, the formation of CO<sub>2</sub> from coals could be due to the existence of intramolecular carboxylic acid anhydrides and decomposition

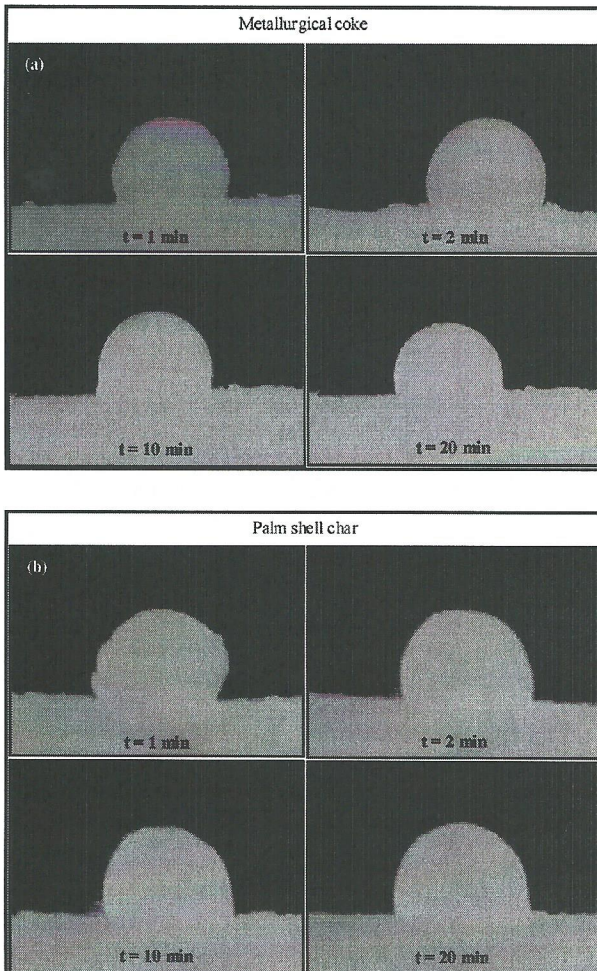


**Figure 5.** Snapshots of slag droplets in contact with (a) raw MC and (b) palm shell char at 1550 °C as a function of time.

of carbonates.<sup>43</sup> The considerable amount of gases evolved from the present carbonaceous materials can be used for subsequent slag–carbon reactions. However, the rate of evolution is known to play an important role because a slower rate leads to a steady release of gases that support stable foam.

**3.2.2. Slag Foaming.** As the carbonaceous substrate/sludge assembly was placed in the hot zone of the furnace, the slag powder melted almost immediately and began reacting with the substrate, releasing CO and CO<sub>2</sub>. The reaction between carbon present in the carbonaceous material and iron oxide in the slag leads to the formation of CO and CO<sub>2</sub> gases, which are entrapped in the slag phase and subsequently released. The carbon/sludge interactions were recorded for 30 min. To qualitatively visualize the foaming phenomena, representative images of the slag droplet with MC and palm shell char are shown in panels a and b of Figure 5. The size of the slag droplet in contact with MC (Figure 5a) did not show a significant variation with time during the initial stages. After 10 min of reaction, the slag droplet fluctuated to a small extent and maintained a reasonably spherical shape. In the case of palm shell char, an increased volume was observed, followed by multiple fluctuations, indicating an improvement in the slag volume (Figure 5b).

323  
324  
325  
326  
327  
328  
329  
330  
331  
332  
333  
334  
335  
336  
337  
338 F5  
339  
340  
341  
342  
343  
344

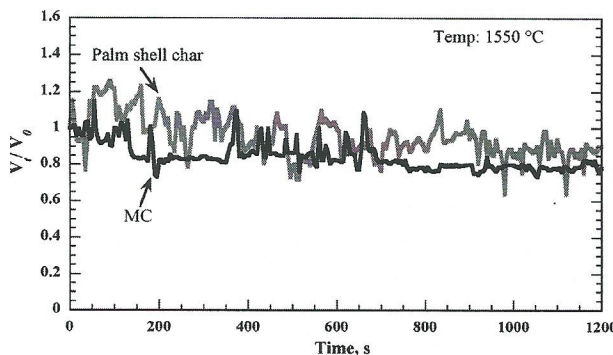


**Figure 6.** Carbon/slag interactions for the MC/slag and palm shell char/slag systems at 1550 °C: volume ratio ( $V_t/V_0$ ) as a function of time.

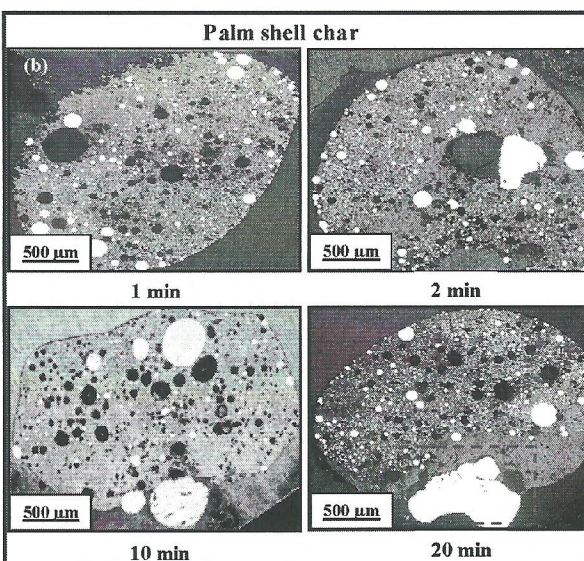
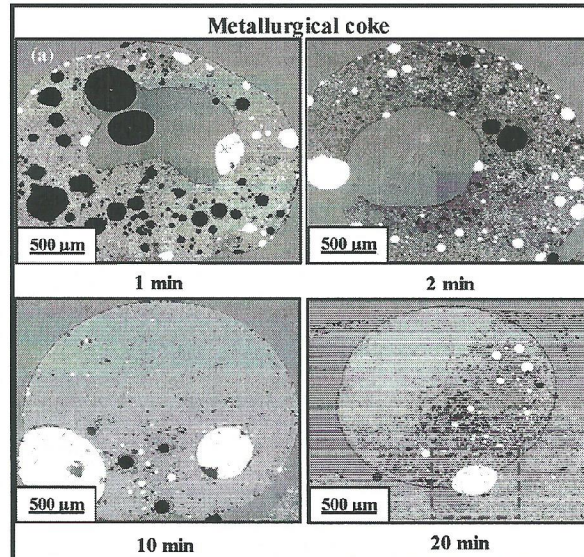
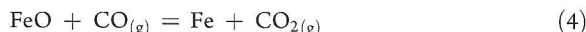
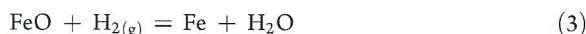


**Figure 7.** Optical microscopy results on quenched (a) MC/slag and (b) palm shell char/slag at 1550 °C. Bright regions represent reduced iron droplets. Trapped gas bubbles are represented by dark spots.

This result may be attributed to the presence of hydrogen that is known to promote gas formation at high temperatures. Hydrogen gas can reduce the iron oxide present in the slag at a faster rate than carbon monoxide and solid carbon.



The reduction of FeO by H<sub>2</sub> and CO will produce CO<sub>2</sub> and H<sub>2</sub>O. Moreover, eq 1 will gasify any available carbon at high temperatures; thus, the key advantage of palm shell comes from its increased hydrogen content, in comparison to MC.

**3.2.3. Volume Ratio Measurements.** Gas hold-up in the slag droplet was measured in terms of  $V_t/V_0$ , where  $V_t$  is the volume of the slag droplet at time  $t$  and  $V_0$  is the initial slag volume (Figure 6). The initial slag melting stage is represented by  $t = 0$  and a volume ratio equal to 1. Changes are observed corresponding to CO and CO<sub>2</sub> generation and entrapment. After a certain period of time, gas activity has reduced considerably and  $V_t/V_0$  is seen to stabilize.

From Figure 6, the palm shell char has a significant variation in volume ratios, with the volume ratio fluctuating between 1.0 and 1.3 for the first 100 s and between 1.0 and 1.2 after 200 s. This indicates that the decrease in the slag volume took longer when palm shell char was used, suggesting significant levels of gas entrapment and subsequent release during carbon/slag interactions. MC has the volume ratio in the range of 0.8–1.0. After 600 s, the size of the bubbles decreased considerably to 0.7, indicating a lower extent of gas entrapment by the slag. The results suggest the potential of palm shell char injection to give immediate and observable differences to slag foaming, increasing foam volume. The method and experimental setup (sessile-drop technique) used here were previously studied by Rahman and Sahajwalla et al.<sup>25,46</sup> and have been successfully applied to compare a wide range of materials.

**3.2.4. Microscopic Investigations.** Optical micrographs of the quenched samples during reactions at different times were investigated to develop an understanding of the role of the gas entrapment on slag foaming (Figure 7). Extensive reduction of iron oxide (Figure 7a) was observed after 1 min of contact when the EAF slag was put in contact with coke. A large number of molten iron droplets (shiny round particles) were also observed dispersed throughout the slag matrix, sitting either at the carbon/slag or gas/slag interface. Gas bubbles trapped within the slag droplet were generally quite small in size. After 10 min of contact,

the reduced iron in the slag droplet was seen precipitated on the substrate.

A close inspection of the cross-section of the slag/palm shell char sample revealed a different behavior. From Figure 7b, we observe a large number of small-diameter gas bubbles dispersed throughout the entire slag volume. Thus, the overall slag volume is dictated by the large number of small gas bubbles. With an increasing reaction time, small-diameter gas bubbles were still present; however, their numbers were greatly reduced. At the latter stages of the reaction, the reduction was complete, with the molten metal resting at the interface appearing as a bright round shiny droplet (marked in Figure 7).

Tables 4 and 5 show the bubble diameters as measured from the optical images for MC/slag and palm shell char/slag samples

387  
388  
389  
390  
391  
392  
393  
394  
395  
396  
397  
398  
399 T4  
400 TS

**Table 4. Minimum Bubble Diameter in Slag Droplets in Contact with MC and Palm Shell Char**

| sample          | minimum bubble diameter ( $\mu\text{m}$ ) |       |        |
|-----------------|---|-------|--------|
|                 | 1 min                                     | 2 min | 10 min |
| MC              | 111.2                                     | 111.0 | 83.3   |
| palm shell char | 55.6                                      | 55.8  | 55.5   |

**Table 5. Maximum Bubble Diameter in Slag Droplets in Contact with MC and Palm Shell Char**

| sample          | maximum bubble diameter ( $\mu\text{m}$ ) |       |        |
|-----------------|---|-------|--------|
|                 | 1 min                                     | 2 min | 10 min |
| MC              | 498.5                                     | 250.5 | 194.6  |
| palm shell char | 388.9                                     | 400.5 | 277.8  |

at different times. The quantitative estimation was carried out using the scale marked on the optical microscopic images. The minimum bubble diameters observed for palm shell char were generally smaller than the corresponding values measured for MC. Because of their better retention, these smaller bubbles are expected to improve slag foaming. These results are consistent with previous research, where the minimum size gas bubbles found in the slag after the reaction with rubber–coke blends led to improved foaming.<sup>18,47</sup> Teasdale and Hayes<sup>48</sup> proposed a gas ferrying mechanism, wherein CO gas produced in the initial reaction between carbon and slag becomes transported through the gas phase and reacts with iron oxide in slag to produce CO<sub>2</sub> and metallic iron. This CO<sub>2</sub> is ferried back to carbon, where gasification of CO<sub>2</sub> to CO takes place via the Boudouard reaction. Gas entrapment in slags as a result of carbon/slag interactions is a dynamic phenomena depending upon a number of physical and chemical factors. In addition, ash oxides present in the substrate can also participate in the reduction reaction and associated gas generation. These could also account for excess CO and CO<sub>2</sub> generated.<sup>25</sup>

Our results indicate that the fundamental properties of the carbonaceous materials and their interactions with slag effectively control interfacial reactions between carbon and slag. These are essential for maintaining sustained slag foaming through gas generation and subsequent retention of trapped gas bubbles within the slag.

#### 4. CONCLUSION

This study has shown that palm shell char could be used to partially replace some of the conventional carbon materials used as injectants in EAF steelmaking. Key results are summarized below: (1) At temperatures above 1000 °C, the gas products evolving from palm shell pyrolysis measured by TGA–MS showed CO, CO<sub>2</sub>, and H<sub>2</sub> as the main gases. These were attributed to the lignocellulosic structure present in palm shells, allowing for a steady gas release for participation in the subsequent carbon/slag interactions. (2) Significant carbon/slag interactions occurred when palm shell char was used compared to the conventional coke because the gases evolving from MC showed lower concentrations of CO compared to palm shell. (3) An increase in the slag volume and fluctuations were observed when palm char reacted with the EAF slag, while coke showed a low

degree of fluctuations and poor volume ratios. (4) Optical microscopic investigations showed the presence of small-diameter gas bubbles trapped within the slag after contact with palm char. These results were in good agreement with the volume measurements.

#### ■ AUTHOR INFORMATION

##### Corresponding Author

\*Telephone: +61293857566. Fax: +61293854292. E-mail: n.f.mohdyunos@student.unsw.edu.au.

#### ■ ACKNOWLEDGMENT

Financial support for the Ph.D. student, Nur Farhana M. Yunos, was provided by the Ministry of Higher Education, Malaysia.

#### ■ REFERENCES

- (1) Chor, L. Y. *Leveraging on Sustainability*; Malaysian Palm Oil Institute: Kuala Lumpur, Malaysia, 2010.
- (2) Azri, S. M. Pyrolysis of empty oil palm fruit bunches using the quartz fluidised-fixed bed reactor. M.Sc. Thesis, University of Malaya, Kuala Lumpur, Malaysia, 2008.
- (3) Harada, T.; Tanaka, H. *ISIJ Int.* 2011, 51 (8), 1301–1307.
- (4) Mandil, C. *Prospects for CO<sub>2</sub> Capture and Storage*; International Energy Agency: Paris, France, 2004.
- (5) Orth, A.; Anastasijevic, N.; Eichberger, H. *Miner. Eng.* 2007, 20 (9), 854–861.
- (6) Gupta, R. C. *Miner. Process. Extr. Metall. Rev.* 2003, 24 (3), 203–231.
- (7) Burgess, J. *Proceedings of the Green Processing Conference, AusIMM*; Melbourne, Victoria, Australia, 2004; p 9.
- (8) Dell'Amico, M.; Fung, P.; Lovel, R.; Manuel, J.; O'Connor, M. *Proceedings of the Green Processing Conference, AusIMM*; Melbourne, Victoria, Australia, 2004; p 73.
- (9) Macedo, C.; d'Avila, E. A. O.; Brosnan, J. G. *Proceedings of the Electric Furnace Conference*; Atlanta, GA, 1985; pp 255–261.
- (10) Coates, K. *Millennium Steel* 2007, 57–60.
- (11) Babich, A.; Senk, D.; Fernandez, M. *ISIJ Int.* 2010, 50 (1), 81–88.
- (12) Emmerich, F. G.; Luengo, C. A. *Biomass Bioenergy* 1996, 10 (1), 41–44.
- (13) Emmerich, F. G.; Luengo, C. A. *Fuel* 1994, 73 (7), 1235–1236.
- (14) Watanabe, K.; Ueda, S.; Inoue, R.; Ariyama, T. *ISIJ Int.* 2010, 50 (4), 524–530.
- (15) Motlagh, M. *I&SM, Iron Steelmaker* 1991, 18 (10), 73–78.
- (16) Bisio, G.; Rubatto, G. *Energy Convers. Manage.* 2002, 43 (2), 205–220.
- (17) Sánchez-Pérez, R.; García-Demedices, L.; Ramos, J.; Díaz-Cruz, M.; Morales, R. *Metall. Mater. Trans. B* 2004, 35 (1), 85–99.
- (18) Ramos-Banderas, A.; Morales, R. D.; Sánchez-Pérez, R.; García-Demedices, L.; Solorio-Díaz, G. *Int. J. Multiphase Flow* 2005, 31 (5), 643–665.
- (19) Bikerman, J. J.; Perri, J.; Booth, R. *Foams: Theory and Industrial Applications*; Reinhold: New York, 1953.
- (20) Sun, H.; Easman, W. *Energy Fuels* 2007, 21, 413–418.
- (21) Zaharia, M.; Sahajwalla, V.; Khanna, R.; Kosyi, P.; O'Kane, P. *ISIJ Int.* 2009, 49 (10), 1513–1521.
- (22) Sahajwalla, V.; Rahman, M.; Khanna, R.; Saha-Chaudhury, N.; O'Kane, P. *Steel Res. Int.* 2009, 80 (8), 535–543.
- (23) Zaharia, M.; Sahajwalla, V.; Kim, B.-C.; Khanna, R.; Saha-Chaudhury, N.; O'Kane, P.; Dicker, J.; Skidmore, C.; Knights, D. *Energy Fuels* 2009, 23 (5), 2467–2474.
- (24) Sahajwalla, V.; Zaharia, M.; Antony, A. A. A.; Lee, J.; Darma, S.; Khanna, R. *Proceedings of the AISTech—Iron and Steel Technology Conference*; Cleveland, OH, 2006.

- 503 (25) Rahman, M.; Khanna, R.; Sahajwalla, V.; O'Kane, P. *ISIJ Int.*  
504 2009, 49 (3), 329–336.  
505 (26) Sahajwalla, V.; Mehta, A. S.; Khanna, R. *Metall. Mater. Trans. B*  
506 2004, 35 (1), 75.  
507 (27) Khanna, R.; Mahfuzur, R.; Richard, L.; Veena, S. *Metall. Mater.*  
508 *Trans. B* 2007, 38 (4), 719–723.  
509 (28) Morales, R. D.; Lule, R.; Lopez, F.; Camacho, J.; Romero, A.  
510 *ISIJ Int.* 1995, 35 (9), 1054–1062.  
511 (29) Chambrion, P.; Orikasa, H.; Suzuki, T.; Kyotani, T.; Tomita, A.  
512 *Fuel* 1997, 76 (6), 493–498.  
513 (30) Din, A. T. M.; Hameed, B. H.; Ahmad, A. L. *Eng. J. Univ. Qatar*  
514 2005, 18, 57–66.  
515 (31) Yang, H.; Yan, R.; Chen, H.; Lee, D. H.; Zheng, C. *Fuel* 2007, 86  
516 (12–13), 1781–1788.  
517 (32) Yang, H.; Yan, R.; Chin, T.; Liang, D. T.; Chen, H.; Zheng, C.  
518 *Energy Fuels* 2004, 18 (6), 1814–1821.  
519 (33) Di Blasi, C.; Signorelli, G.; Di Russo, C.; Rea, G. *Ind. Eng. Chem.*  
520 *Res.* 1999, 38 (6), 2216–2224.  
521 (34) Worasuwannarak, N.; Sonobe, T.; Tanthapanichakoon, W.  
522 *J. Anal. Appl. Pyrolysis* 2007, 78 (2), 265–271.  
523 (35) Cagigas, A.; Escudero, J. B.; Low, M. J. D.; Pis, J. J.; Tascon,  
524 J. M. D. *Fuel Process. Technol.* 1987, 15, 245–256.  
525 (36) Serio, M. A.; Hamblen, D. G.; Markham, J. R.; Solomon, P. R.  
526 *Energy Fuels* 1987, 1 (2), 138–152.  
527 (37) Hasegawa, I.; Tabata, K.; Okuma, O.; Mae, K. *Energy Fuels*  
528 2004, 18 (3), 755–760.  
529 (38) Yang, H.; Yan, R.; Chen, H.; Lee, D. H.; Liang, D. T.; Zheng, C.  
530 *Energy Fuels* 2006, 20 (3), 1321–1328.  
531 (39) Yunos, N. F. M.; Zaharia, M.; Ahmad, A. K.; Nath, D.; Iwase,  
532 M.; Sahajwalla, V. *ISIJ Int.* 2011, 51 (7), 1185–1193.  
533 (40) Hosoya, T.; Kawamoto, H.; Saka, S. *J. Wood Sci.* 2007, 53 (4),  
534 351–357.  
535 (41) Dankwah, J. R.; Koshy, P.; Saha-Chaudhury, N. M.; O'Kane, P.;  
536 Skidmore, C.; Knights, D.; Sahajwalla, V. *ISIJ Int.* 2011, 51 (3), 498–507.  
537 (42) Woolley, E.; Larson, H. R.; Pal, U. B.; McLean, A. *Proceedings of*  
538 *the EPD Congress '98*; San Antonio, TX, 1998; p 611.  
539 (43) van Heek, K. H.; Hodek, W. *Fuel* 1994, 73 (6), 886–896.  
540 (44) Gupta, S.; Dubikova, M.; French, D.; Sahajwalla, V. *Energy Fuels*  
541 2007, 21 (2), 1052–1061.  
542 (45) Berkowitz, N. *Chem. Coal* 1985, 504.  
543 (46) Sahajwalla, V.; Zaharia, M.; Rahman, M.; Khanna, R.; Saha-  
544 Chaudhury, N.; O'Kane, P.; Dicker, J.; Skidmore, C.; Knights, D. *Steel Res.*  
545 *Int.* 2011, 82 (5), 566–572.  
546 (47) Zaharia, M. Reactions of waste rubber tyres and polypropylene  
547 plastics with gases and electric arc furnace steelmaking slags. Ph.D.  
548 Thesis, University of New South Wales, Sydney, New South Wales,  
549 Australia, 2010.  
550 (48) Teasdale, S. L.; Hayes, P. C. *ISIJ Int.* 2005, 45 (5), 634–641.